

Electron Temperature Evolution in Expanding Ultracold Neutral Plasmas

P. Gupta, S. Laha, C. E. Simien, H. Gao, J. Castro, and T. C. Killian
Rice University, Department of Physics and Astronomy, Houston, Texas, 77005

T. Pohl

ITAMP, Harvard-Smithsonian Center for Astrophysics, 60 Garden Street, Cambridge, MA 02138
(Dated: September 15, 2021)

We have used the free expansion of ultracold neutral plasmas as a time-resolved probe of electron temperature. A combination of experimental measurements of the ion expansion velocity and numerical simulations characterize the crossover from an elastic-collision regime at low initial Γ_e , which is dominated by adiabatic cooling of the electrons, to the regime of high Γ_e in which inelastic processes drastically heat the electrons. We identify the time scales and relative contributions of various processes, and experimentally show the importance of radiative decay and disorder-induced electron heating for the first time in ultracold neutral plasmas.

Ultracold neutral plasmas (UNPs) [1] occupy an exotic regime of plasma physics in which electron and ion temperatures are orders of magnitude colder than in conventional neutral plasmas. The electron temperature in these systems evolves under the influence of many factors, which can occur on very different time scales, such as disorder-induced heating [2], three-body recombination [3], and adiabatic cooling [4, 5]. The relative importance of the various effects depends critically upon initial conditions, and this has complicated the experimental study of the electron temperature [6, 7, 8, 9, 10] and lead to much theoretical debate [2, 4, 5, 11, 12]. We present here detailed experimental measurements and numerical simulations that untangle the time scales and contributions of the various competing effects and characterize the transition from elastic-collision-dominated to inelastic-collision-dominated behavior.

UNPs are of fundamental interest because they can be in or near the strongly coupled regime, which is characterized by the existence of spatial correlations between particles and a Coulomb coupling parameter $\Gamma = e^2/(4\pi\epsilon_0 ak_B T) > 1$, where T refers to the temperature of the particles and $a = (4\pi n/3)^{-1/3}$ is the Wigner-Seitz radius. Ions in UNPs equilibrate with $\Gamma_i \sim 3$ [8, 13]. The initial electron temperature is under experimental control and can be set such that a naive calculation of Γ_e suggests that electrons are also strongly coupled. However, electrons rapidly leave the strongly coupled regime due to various heating mechanisms [2, 5, 12] that are central to studies presented here.

UNPs are created by photoionizing laser-cooled Sr atoms [14] just above the ionization threshold with a 10 ns laser pulse. The ion temperature is initially a few millikelvin, which is similar to the temperature of the laser-cooled neutral atoms, but ions heat within one microsecond to about 1 K due to disorder-induced heating [13, 15]. The initial electron kinetic energy (E_e) equals the difference between the energy of the ionizing photon and the ionization threshold. With a tunable pulsed-dye laser, $2E_e/3k_B$ can be set from 1-1000 K. Electrons ther-

malize locally within 100 ns and globally within $1 \mu\text{s}$ [5]. Simple equilibration would set the initial $T_e = 2E_e/3k_B$, but we will discuss processes that can change T_e .

The plasma density follows the profile of the neutral atom cloud. By adjusting the laser-cooling parameters and imaging the cloud in two perpendicular axes, we ensure that the plasma has a spherically symmetric Gaussian profile, $n(r) = n_0 e^{-r^2/2\sigma^2}$. Deviations from spherical symmetry, *e.g.* $(\sigma_x - \sigma_y)/\sigma_x$, are less than 5%. Typically, the initial n_0 is $\sim 10^{16} \text{ m}^{-3}$ and $\sigma \sim 1 \text{ mm}$. The plasma is quasineutral ($n_i \sim n_e$) with the Debye length $\lambda_D = (\epsilon_0 k_B T_e / n_e e^2)^{1/2} \ll \sigma$, where n_i and n_e refer to ion and electron density respectively. UNPs are unconfined and expand into the surrounding vacuum, and quasineutrality is maintained during the expansion.

Electron temperature evolution during expansion of ultracold plasmas has been studied using various techniques. Electron plasma oscillations [6] measured the average density in order to obtain the rms radial terminal velocity of the ions. This showed that essentially all the initial electron energy is converted to ion expansion energy. In addition, plasmas with lower E_e and higher n_0 (which would imply $\Gamma_e \gtrsim 1$ [16]) resulted in an anomalously fast expansion. Numerical simulations [5] showed that various electron heating mechanisms explained the result. However, the relationship between density and the electron plasma oscillation used in [6] has been called into question in subsequent work [10, 17]. Ref. [7] probed T_e by measuring the fraction of electrons escaping the plasma during a small electric field pulse and inferred that for $10 \text{ K} < 2E_e/3k_B < 300 \text{ K}$ and $n_0 \sim 5 \times 10^{14} \text{ m}^{-3}$, electrons approach a narrow range of electron temperatures ($20 \text{ K} < T_e < 40 \text{ K}$) about $5 \mu\text{s}$ after photoionization. Spatially resolved fluorescence detection of the ions [8, 9] in a cylindrical plasma measured expansion energies similar to what was observed in [6], but they found significant deviations from theoretical predictions that perhaps arose because of the lack of spherical symmetry. Tonks-Dattner modes, which have resonant frequencies that are sensitive to T_e , were recently observed in UNPs

[10]. They found agreement between data and a model that assumed constant T_e over $40 \mu\text{s}$ of evolution. So the electron temperature evolution in UNPs is obviously a complicated problem that remains unsettled.

The results presented here have several advantages over previous studies. We have a spherically symmetric plasma that allows the application of exact analytic results. Doppler broadening of the ion optical absorption spectrum [13] provides a calibrated, model-independent measure of the ion velocity and overall plasma expansion with excellent temporal resolution stretching from the phase of initial ion acceleration to the onset of terminal velocity. A combination of experiment and numerical simulation allows the contributions of various electron heating and cooling mechanisms to be separated as never before, and we find excellent agreement between experiment and theory with no adjustable parameters. We also present a systematic study of the full spectrum of dynamics observed in current UNP experiments.

For an experimental probe, the Doppler width of the ion absorption spectrum [13] for the entire plasma measures $\sqrt{\langle(\mathbf{v} \cdot \hat{\mathbf{z}})^2\rangle} \equiv v_{i,rms}$ [18], where $\hat{\mathbf{z}}$ is the laser propagation direction, \mathbf{v} is the total ion velocity including random thermal motion and expansion (\mathbf{u}), the angled brackets refer to an average over the plasma density and velocity distribution. In a quasineutral Gaussian plasma such as a UNP, the electron temperature can be found from measurements of $v_{i,rms}$ due to its sensitivity to \mathbf{u} and the fact that the expansion acceleration,

$$\dot{\mathbf{u}} = -\frac{k_B(T_e + T_i)}{m_i} \frac{\nabla n}{n}, \quad (1)$$

arises from thermal pressure [4, 5, 6, 20].

For high E_e and low n_0 , which we denote as the “elastic collisional regime” ($\Gamma_e < 0.1$ [16]), all collisional processes in a UNP are elastic, the plasma expands adiabatically, and electrons cool [21]. This leads to a self-similar expansion that preserves the Gaussian phase-space distributions and is described by an analytic solution of the Vlasov equations [4, 5] that was originally derived for short-pulse laser experiments [20, 22, 23] and applied to UNPs in [4, 5]. UNPs provide the first clean realization of this analytic solution, and this was shown experimentally in [24]. The Vlasov equations do not include a collision term, which is appropriate because such a term vanishes for a Maxwell-Boltzmann velocity distribution. So in this sense, the expansion in the elastic collisional regime can also be called “collisionless” [20].

In this regime, $v_{i,rms}$ is given by [24]

$$v_{i,rms} = \sqrt{\frac{k_B}{m_i \tau_{exp}^2} [t^2 (T_e + T_i) + \tau_{exp}^2 T_i]}. \quad (2)$$

The characteristic expansion time τ_{exp} is given by $\tau_{exp} = \sqrt{m_i \sigma(0)^2 / k_B [T_e(0) + T_i(0)]}$, and the electron and ion

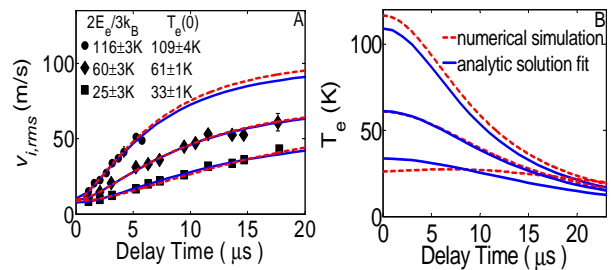


FIG. 1: Expansion velocity (A) and electron temperature (B) for low Γ_e showing little or no electron heating effects. (A) The initial peak densities and sizes are $n_0 = 3.5 \times 10^{15} \text{ m}^{-3}$ and $\sigma(0) = 1 \text{ mm}$. The self-similar analytic solution (dark solid line) provides an excellent fit of the data, with fit $T_e(0)$ indicated in the legend. The full numerical simulation (dashed line) describes the data with no adjustable parameters. (B) Electron temperature evolutions (Eq. 3) are determined from parameters of the fits to $v_{i,rms}$ or by numerical simulation. For $2E_e/3k_B = 25 \text{ K}$, the analytic solution fit and numerical simulation for $T_e(t)$ deviate significantly, showing the importance of inelastic collision effects.

temperatures follow

$$T_{e/i} = T_{e/i}(0) / (1 + t^2 / \tau_{exp}^2). \quad (3)$$

Figure 1A shows the ion velocity evolution for UNPs in the elastic collisional regime. Fits using Eq. 2 take $T_{i/e}(0)$ as fit parameters, while $\sigma(0)$ is fixed to the value found from the images. For higher E_e in Fig. 1, the fit is excellent and the extracted values of $T_e(0)$ yield $2E_e/3k_B$ within experimental uncertainty, confirming that inelastic collisions are negligible in this regime. The underlying electron temperature evolution is shown in Fig. 1B. As expected, T_e drops due to adiabatic cooling because there is no significant electron heating.

For $2E_e/3k_B = 25 \text{ K}$ in Fig. 1, the fit $T_e(0) = 33 \text{ K}$ exceeds the expected value. This provides evidence that inelastic processes are modifying the electron temperature. Many processes are expected to contribute. Within tens of nanoseconds, disorder-induced heating (DIH) [2, 25] increases electron kinetic energy by as much as several kelvin above E_e in the range of our initial conditions. DIH is the conversion of potential energy into kinetic as spatial correlations develop, which is an effect of strong coupling that has been observed for ions in UNPs [13]. Three-body recombination (TBR) [3] populates Rydberg levels bound by $\sim k_B T_e$ and heats the free electrons. The total TBR rate varies as $T_e^{-9/2}$ and can be very rapid in ultracold systems [26]. Rydberg-electron collisions (REC) [3, 5] can transfer Rydberg atoms to more deeply bound levels and heat electrons further, while radiative decay (RD) of the Rydberg atoms mitigates this heating effect. Direct cooling of electrons through equilibration with ions is negligibly slow for these experiments because of the large ion-electron mass difference [27].

To understand the interplay between these various ef-

fects, we performed numerical simulations, taking into account all relevant heating and cooling mechanisms. Our description is based on a particle-in-cell simulation of the ions and treats the electrons adiabatically as a fluid in a constantly changing equilibrium state [4, 5]. DIH due to particle correlations is accounted for in the initial conditions of both plasma components [2, 15], assuming a homogeneous T_e for the electrons and a homogeneous Γ_i for the ions. This treatment neglects the influence of correlations on later stages of the plasma dynamics, which may be a concern because UNP ions are strongly coupled [8, 13], but [4] showed that the effects of ion-ion correlations on the expansion are negligible. Finally we use a Monte-Carlo treatment to describe the formation of Rydberg atoms and their subsequent binding energy evolution, employing known expressions for the rates of TBR and REC [3] and RD [28]. The TBR rates [3] are well-confirmed experimentally at high temperatures, but their low temperature validity has been questioned [29, 30, 31] as it ultimately has to break down for $T_e \rightarrow 0$ due to its strong $\propto T_e^{-9/2}$ temperature divergence. By comparing experiments and calculations the present study indirectly tests TBR theory over a wide range of temperatures.

The numerical simulation reproduces the expansion dynamics in Fig. 1 with no adjustable parameters, and it shows that $2E_e/3k_B = 25$ K is on the border of the “inelastic collisional regime”, which is defined here as initial $\Gamma_e > 0.1$ [16]. For this data set, $T_e(t)$ stays roughly constant over the observed evolution time and is not well-described by the analytic solution (Eq. 3). Only TBR and REC processes must be included in the simulation to accurately describe the expansion.

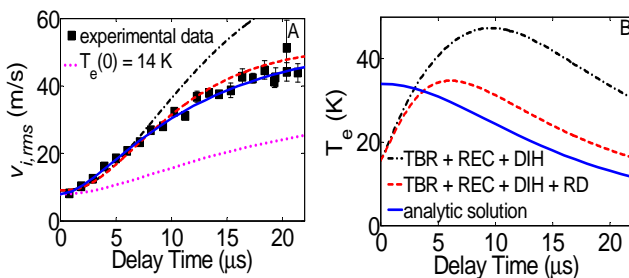


FIG. 2: (A) Expansion velocity and (B) electron temperature (B) for moderate initial $\Gamma_e = 0.2$, ($2E_e/3k_B = 14$ K, $\sigma(0) = 0.9$ mm, and $n_0(0) = 7 \times 10^{15} \text{ m}^{-3}$). (A) A fit of the expansion to the analytic solution (Eq. 2, solid line) yields $T_e(0) = 34$ K, which reflects much faster expansion than expected for elastic-collisional dynamics with $2E_e/3k_B = 14$ K (dotted line). Only including TBR and REC in the simulation (dot-dash line) overestimates the heating. Including RD as well (dashed line) brings theory into good agreement with experiment. Including DIH increases the initial electron temperature by about 3 K, but has little effect on the velocity fit. (B) The fit $T_e(0)$ approximately equals the maximum of the actual $T_e(t)$ obtained with simulation.

Fig. 2A displays characteristic plasma dynamics for a

UNP with lower initial electron energy and higher Γ_e that is in the inelastic collisional regime. The expansion is much faster than expected for elastic-collisional-regime dynamics with $T_e(0) = 2E_e/3k_B = 14$ K. Incorporating only TBR and REC in the simulation considerably overshoots the observed ion velocity evolution because it overestimates electron heating. Inclusion of RD, which transfers Rydberg atoms to more deeply bound states without heating the plasma electrons, produces excellent agreement with experiment without adjustable parameters.

The analytic solution (Eq. 2) provides a surprisingly accurate description of observed ion velocities, but the simulation shows (Fig. 2B) that the extracted $T_e(0)$ is only a phenomenological parameter. Physically, TBR and REC heat the electrons in the first $\sim 5 \mu\text{s}$, although it is mitigated by RD. The increasing T_e , and to a lesser extent decreasing density, slows TBR, so that adiabatic cooling dominates at later times. The fit $T_e(0)$ gives a rough estimate of the maximum electron temperature, $T_{e,max}$.

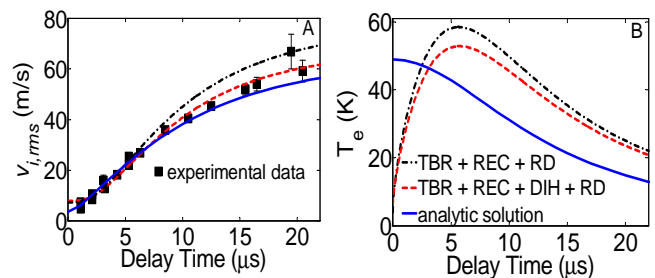


FIG. 3: (A) Ion velocity and (B) electron temperature for $\Gamma_e \sim 1$, ($2E_e/3k_B = 4$ K, $n_0(0) = 8 \times 10^{15} \text{ cm}^{-3}$, $\sigma(0) = 1.0$ mm). (A) The numerical simulation including all heating effects matches the data with no adjustable parameters. For this relatively high density, the initial heating from DIH slows TBR and REC enough to produce an observable effect. The analytic solution fit is poor, but yields $T_e(0) = 49 \pm 2$ K. (B) The electron temperature shows drastic heating at early times and $T_e(0)$ no longer provides a good estimate of $T_{e,max}$.

Further decrease of E_e or increase in density pushes further into the inelastic collisional regime where a naive calculation using $T_e = 2E_e/3k_B$ implies $\Gamma_e \gtrsim 1$. In this regime, fits using the analytic expansion expression fail to reproduce the data (Fig. 3). Simulations show that the approximation of a self-similar Gaussian expansion also becomes poor due to the large fraction of ions that undergo TBR and the higher rate for this process in the higher density central region of the plasma. The measured ion expansion velocity indicates the occurrence of extreme electron heating from $2E_e/3k_B = 4$ K. For this relatively high-density sample DIH makes a significant contribution. It quickly raises T_e , which slows recombination and leads to a lower $T_{e,max} = 53$ K. The agreement between data and simulation indicates no significant de-

viation from classical TBR theory [3].

Figure 4 summarizes our results for electron heating in UNPs. The data is organized according to initial Γ_e [16], and it displays a clear trend in the heating of the electrons as previously observed in [6, 9]. The onset of heating occurs at the crossover between the inelastic and elastic collisional regime. For initial $\Gamma_e \gtrsim 1$, the expansion ceases to be self-similar.

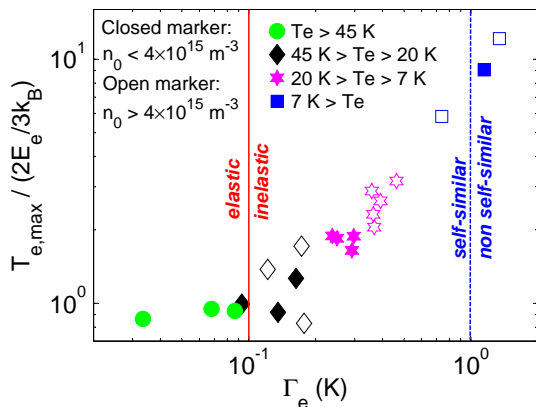


FIG. 4: Electron heating summary. The plasma dynamics are parameterized well by $\Gamma_e(n_0, E_e)$. $T_{e,max}$ is the maximum electron temperature attained during the evolution. The heating is negligible in the elastic collisional regime ($\Gamma_e < 0.1$ [16]), and $T_{e,max}/(2E_e/3k_B) \approx 1$. In the inelastic collisional regime, the heating becomes significant and increases with increasing density and decreasing $2E_e/3k_B$. Beyond $\Gamma_e \approx 1$, the expansion ceases to be self-similar.

We have described the use of spectroscopic measurements of the ion velocity and numerical simulations as a time-resolved probe of the electron dynamics of UNPs. It resolves outstanding questions regarding the evolution of the electron temperature, and shows that the dynamics vary greatly for different initial electron kinetic energy and plasma density. This work identifies the relative contributions and timescales of various processes, demonstrates the importance of radiative decay and disorder-induced electron heating for the first time in UNPs, and shows no discrepancy between observed and theoretical rates of TBR.

This work was supported by the National Science Foundation (Grant PHY-0355069 and a grant for the Institute of Theoretical Atomic, Molecular and Optical Physics (ITAMP) at Harvard University and Smithsonian Astrophysical Observatory) and the David and Lucille Packard Foundation.

- [2] S. G. Kuzmin and T. M. O’Neil, *Phys. Plasmas* **9**, 3743 (2002).
- [3] P. Mansbach and J. Keck, *Phys. Rev.* **181**, 275 (1969).
- [4] T. Pohl, T. Pattard, and J. M. Rost, *Phys. Rev. A* **70**, 033416 (2004).
- [5] F. Robicheaux and J. D. Hanson, *Phys. Plasmas* **10**, 2217 (2003).
- [6] S. Kulin, T. C. Killian, S. D. Bergeson, and S. L. Rolston, *Phys. Rev. Lett.* **85**, 318 (2000).
- [7] J. L. Roberts, C. D. Fertig, M. J. Lim, and S. L. Rolston, *Phys. Rev. Lett.* **92**, 253003 (2004).
- [8] E. A. Cummings, J. E. Daily, D. S. Durfee, and S. D. Bergeson, *Phys. Rev. Lett.* **95**, 235001 (2005).
- [9] E. A. Cummings, J. E. Daily, D. S. Durfee, and S. D. Bergeson, *Phys. Plasmas* **12**, 123501 (2005).
- [10] R. S. Fletcher, X. L. Zhang, and S. L. Rolston, *Phys. Rev. Lett.* **96**, 105003 (2006).
- [11] A. N. Tkachev and S. I. Yakovlenko, *Quantum Electronics* **30**, 1077 (2000).
- [12] S. Mazevet, L. A. Collins, and J. D. Kress, *Phys. Rev. Lett.* **88**, 55001 (2002).
- [13] C. E. Simien et al., *Phys. Rev. Lett.* **92**, 143001 (2004).
- [14] S. B. Nagel et al., *Phys. Rev. A* **67**, 011401 (2003).
- [15] M. S. Murillo, *Phys. Rev. Lett.* **87**, 115003 (2001).
- [16] For characterizing dynamics according to initial conditions, Γ_e is calculated using initial peak density and the naive assumption of initial $T_e = 2E_e/3k_B$. The plasma may be far from thermal equilibrium at these early times.
- [17] S. D. Bergeson and R. L. Spencer, *Phys. Rev. E* **67**, 026414 (2003).
- [18] This is rigorously true for a self-similar expansion and uniform ion temperature. It is a good approximation in the absence of these conditions [19].
- [19] T. C. Killian et al., *J. Phys. B: At. Mol. Opt. Phys.* **38**, 351 (2005), (Equations 7, 10, 11, and 17 should be multiplied by γ_0/γ_{eff}).
- [20] D. S. Dorozhkina and V. E. Semenov, *Phys. Rev. Lett.* **81**, 2691 (1998).
- [21] T. Pohl, T. Pattard, and J. M. Rost, *Phys. Rev. Lett.* **92**, 155003 (2004).
- [22] A. V. Baitin and K. M. Kuzanyan, *J. Plasma Phys.* **59**, 83 (1998).
- [23] V. F. Kovalev and V. Y. Bychenkov, *Phys. Rev. Lett.* **90**, 185004 (2003).
- [24] S. Laha, P. Gupta, H. Gao, C. E. Simien, J. Castro, and T. C. Killian, submitted (2007).
- [25] Threshold lowering is sometimes also considered, but electron DIH includes this effect because it is related to spatial correlations between particles.
- [26] T. C. Killian et al., *Phys. Rev. Lett.* **86**, 3759 (2001).
- [27] T. Pohl, T. Pattard, and J. Rost, *J. Phys. B* **38**, S343 (2005).
- [28] H. A. Bethe and E. E. Salpeter, *Quantum Mechanics of One- and Two-Electron Atoms*. (Plenum, New York, 1977).
- [29] Y. Hahn, *Phys. Lett. A* **231**, 82 (1997).
- [30] Y. Hahn, *Phys. Lett. A* **264**, 465 (2000).
- [31] S. A. Maiorov, A. N. Tkachev, and S. I. Yakovlenko, *Physica Scripta* **51**, 498 (1998).

[1] T. C. Killian, *Science* **316**, 705 (2007).